Indentation Load Effect on Young's Modulus and Hardness of Porous Sialon Ceramic by Depth Sensing Indentation Tests *

Osman ŞAHIN**

Department of Physics, Art and Science Faculty, Süleyman Demirel University, Isparta, Turkey

(Received 25 April 2007)

Depth sensing indentation (DSI) tests at the range of 200–1800 mN are performed on porous sialon ceramic to determine the indentation load on Young's modulus and hardness values. The Young modulus and hardness (Dynamic and Martens) values are deduced by analysing the unloading segments of the DSI test load-displacement curves using the Oliver–Pharr method. It is found that Young's modulus E_r, the dynamic hardness H_D and the Martens hardness H_M exhibit significant indentation load dependences. The values of Young's modulus and hardness decrease with the increasing indentation load, as a result of indentation load effect. The experimental h_f/h_m ratios lower than the critical value 0.7, with h_m being the maximum penetration depth during loading and h_f the final unloading depth, indicate that our sample shows the work hardening behaviour.

PACS: 62. 20. −x, 62. 20. Dc, 62. 20. Qp

Silicon nitride (Si_3N_4) is a ceramic that has many properties, e.g., resistance to wear, corrosion and thermal shock, high hardness and strength, high temperature of decomposition, a large band gap, good dielectric properties, etc., found to be desirable.[1] The silicon nitride system crystallizes generally in two well-known phases: α- and β-Si_3N_4. The α-phase exhibits a lower density with the β-phase obtained from a transformation from α- to β-phase at high temperatures (approximately 2000 K), where β-phase is more stable than α-phase.[2,3] However, silicon nitride has been, to an extent, superseded by the well-known solid solution SiAlON system. The SiAlON system exhibits the same high temperature properties as silicon nitride, with the additional advantage of higher toughness, improved chemical stability and a greater ease of densification.[4]

Depth-sensing indentation (DSI) test has become a commonly accepted method for measuring the mechanical properties of the materials. This method offers great advantages over the conventional indentation test.[5] We therefore characterize the mechanical properties of porous Sialon ceramic by the DSI tests.

The initial powders were α-Si_3N_4 (H.C.Starck-B7, 10–15wt% of β-Si_3N_4), AlN (H.C.Starck-C), and α-Al_2O_3 prepared from $Al(OH)_3$ by firing at 1200°C (total contaminants less than 0.2 wt%, d_{50}-16 μm, SSA_{BET}-0.8 m^2g^{-1}). The mixture was batched according to $z = 0.5$ in β-$Si_{6-z}Al_zO_zN_{8-z}$ solid solution (α-Si_3N_4 = 91.5 wt%, AlN=2.4 wt%, Al_2O_3 = 6.1 wt%), activated in an MPP-1 planetary mill (TTD, RU) with acceleration of the centrifugal field of 28 g, with silicon nitride balls for 45 min. The resultant powder was dispersed in an azeotropic mixture of 60 vol% methylethylketon (MEK) (Aldrich) and 40 vol% ethanol (POCH). We took 3 wt% of Hypermer KD1 (Imperial Chemical Industries PLC, UK) as a dispersant. The suspension was mixed on the roller bench for 24 h. After drying the powders were crushed with a pestle and mortar, uniaxially cold pressed and finally cold isostatically pressed with 200 MPa. Heating in air at 600°C for 2 h was applied in order to remove the residual polymer dispersant. Green density attained the value of 66%. The pressed tablets were contained within a powder bed of Si_3N_4/BN powder within a BN crucible with a lid. Sintering was carried out in a graphite furnace (Thermal Technology) in flowing nitrogen at temperature of 1600°C for 60 min. The size and mass of the specimens were controlled. The density was determined by the Archimedes technique in distilled water. The resultant ceramic was a porous material (porosity 19.9 vol%, density 2,47 gcm^{-3}). The final phase composition consisted of 39.4 wt% of α-Si_3N_4, 45.4 wt% of β-SiAlON with $z = 0.8$ and 15.2 wt% of O'-SiAlON. Lack of eutectic liquid phase during sintering at 1600°C effected in an incomplete conversion of α-Si_3N_4 to β-SiAlON solid solution. Presence of O'-SiAlON and a slight mass increase (0.2 wt%) after densification showed a limited oxidation of the activated powders during reaction sintering.

Hardness measurements of SiAlON ceramic were performed with a dynamic ultra microhardness tester (Shimadzu, DUH-W201S) with Vickers indenter. For an easier interpretation of mechanical behaviour at various depths, the maximum load was changed at regular intervals ranging from 200 to 1800 mN under a loading/unloading rate of 4.4130 mN/s. After each load, no cracks were observed during Vickers indentation. For a particular load at least five indentation tests were conducted on sample surface to increase the reliability of experimental results.

* Supported by the Turkish State Planning Organization (DPT) under Grant No 2003K120510.

** Email: sahin@fef.sdu.edu.tr and sduosman@gmail.com

©2007 Chinese Physical Society and IOP Publishing Ltd

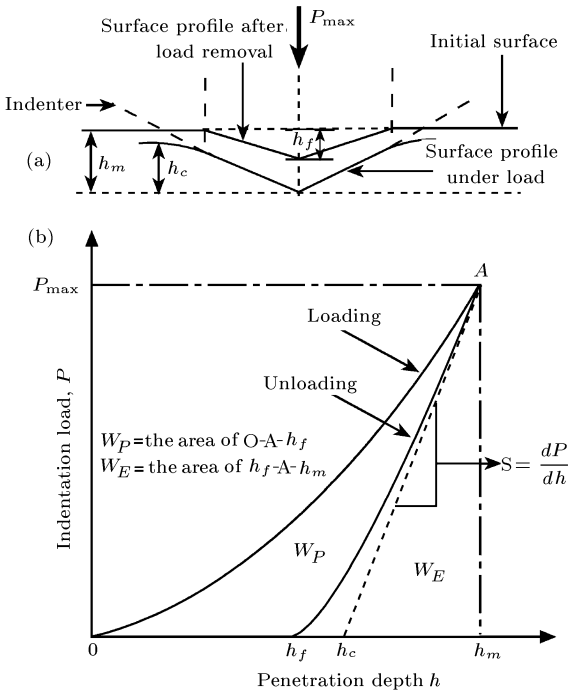

Fig. 1 Schematic plots of a) cross-section of an indentation and b) a typical indentation load-penetration depth curve generated during a depth-sensing indentation experiment, indicating key parameters needed for analysis.

The quantities of interest, which were obtained directly from the raw data or derived from it, include the peak indentation load $P_{\max}$, the maximum penetration depth h_m during loading, the final unloading depth h_f, and the contact depth h_c during unloading, as illustrated in Fig. 1. W_P and W_E are the plastic energy and elastic energy obtained during unloading, respectively, as shown in Fig. 1(b).

The dynamic hardness H_D is calculated by the Oliver–Pharr method,[6] i.e.

$$H_D = \frac{P_{\max}}{A_c} = \frac{P_{\max}}{26.43 h_c^2}, \tag{1}$$

where the contact depth h_c is calculated by $h_c = h_{\max} - \beta \frac{P_{\max}}{dP/dh}$ with β being an constant dependent on indenter geometry. It has been shown that β has an empirical value of 0.75 for the Vickers indenter.[5,7]

We also measured the Martens hardness H_M by the equation

$$H_M = \frac{P_{\max}}{26.43 h_m^2}. \tag{2}$$

On the other hand, the behaviour of the peak indentation test load versus the penetration depth can be effectively used in defining a reduced elastic modulus E_r by the equation

$$\frac{1}{E_r} = \frac{1-\nu_s^2}{E_s} + \frac{1-\nu_i^2}{E_i}, \tag{3}$$

where E and ν are Young's modulus and Poisson's ratio with the subscripts s and i indicating sample and indenter, respectively. E_r is Young's modulus of a sample, given by

$$E_r = \frac{S}{2} \frac{\sqrt{\pi}}{\sqrt{26.43} h_c}. \tag{4}$$

The aforementioned computational procedure can be successfully used to calculate the H_D, H_M and E_r values of the SiAlON ceramic by using the DSI tests.

Figure 2 shows the typical indentation load versus penetration depth curves with the indentation load during DSI tests for the Sialon ceramic. At first glance, one can clearly see that the loading segments of the curves in figure interlink with each other, which points out the similar deformation mechanism for the nine cycles of each indentation experiment. On the other hand, distance between unloading curves decreases with increasing indentation loads. The area of resulting hysteresis loops is a measure of the energy dissipation of irreversible processes occurring during loading to unloading.

The plastic energy W_P and the elastic energy W_E are obtained from the loading and unloading curves based on Fig. 2. Their values increase substantially with increasing load. Figure 3 shows a plot of the plasticity from the plastic energy ratio as a function of the indentation load for the examined sample. The plastic energy ratio is equal to the value of plastic energy divided by the sum of plastic energy and elastic energy. The plastic energy ratio for 200 mN loading is about 58%. However, the plastic energy ratio decreases rapidly as the indentation load increases from 200 to 1800 mN. These results indicate that mechanical properties measured by DSI tests are load dependent. A detailed explanation for the relationship to load dependent behaviour will be given later.

Figure 4 shows the relationship between load over the penetration depth, $P_{\max}/h_c$, and penetration depth h_c curves for the examined material. The plot reveals that good linearity between $P_{\max}/h_c$ and h_c is maintained over the whole range of applied indentation loads. This result proves that the indentation load-size effect on hardness exists in the applied load range. The present linear results are in good agreement with the literature.[8]

Figure 5 shows the influence of the indentation load on the measured Young's moduli. Young's modulus of the specimen is found to be between 94 and 158 GPa. The values of Young's modulus exhibit significant dependence on the indentation test load. Young's moduli tend to decrease with increasing applied load. The decrease of Young's modulus is attributed to the change of slope of unloading and is caused most possibly by microstructural inhomogeneities in the material. It has been reported that Young's modulus of sintered SiC and Si_3N_4 materials decreases with the increasing indentation load.[9]

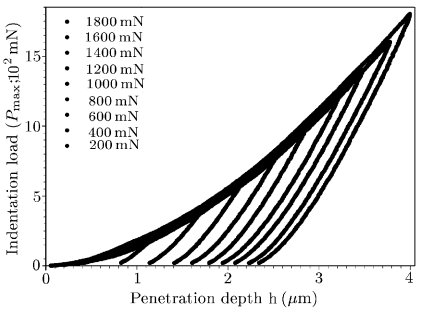

Fig. 2 Indentation load versus penetration depth for Sialon ceramic.

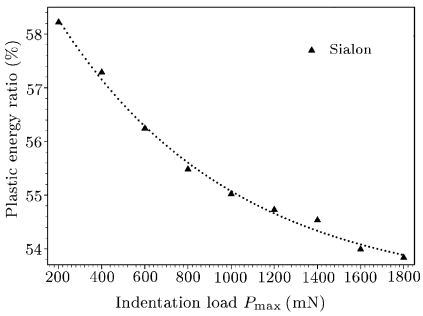

Fig. 3 Relationship between plastic energy ratio and indentation load for Sialon ceramic.

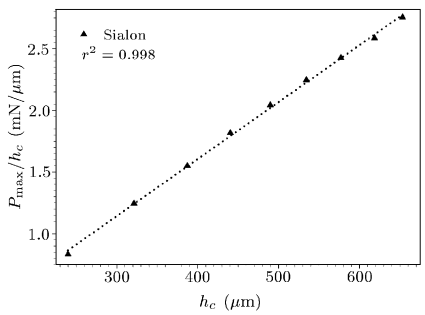

Fig. 4 Relationship between load over the penetration depth (P_{max}/h_c) and penetration depth (h_c) of Sialon ceramic obtained from DSI tests.

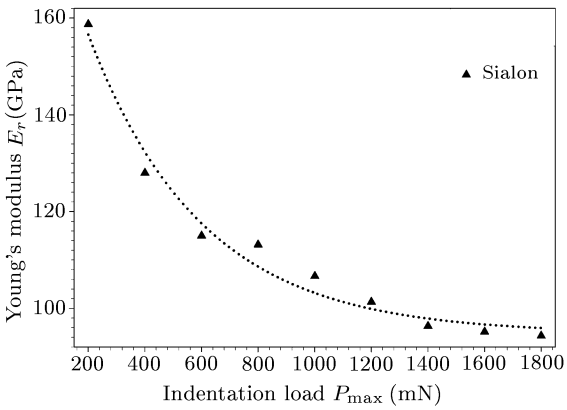

Fig. 5. Young's modulus as a function of indentation load for Sialon ceramic obtained from DSI tests.

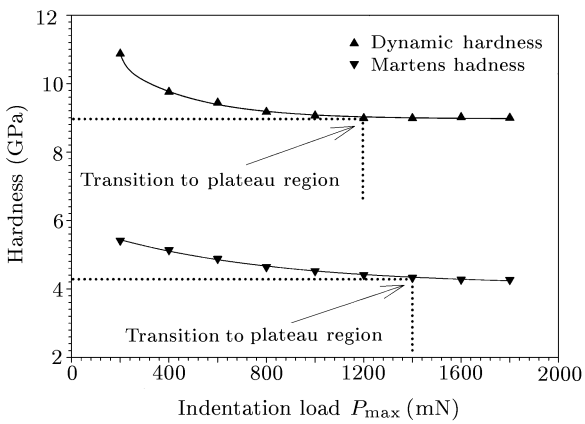

Fig. 6 Dynamic and Martens hardness as a function of indentation load for Sialon ceramic obtained from DSI tests.

Figure 6 shows the influence of indentation load on the measured hardness of the specimen. In the figure, H_M values are compared with the H_D values which are deduced from the relationship between load and the projected area of the indentation impression.[6] It can be seen from that H_D values are significantly higher for all indentation loads than the H_M values. The hardness values of the specimen tend to decrease with increasing indentation load. Consequently, the hardness values reveal a similar tendency to that of the indentation load-size effect observed in Young's modulus values. This trend is consistent with the results reported in the literature.[10] On the other hand, Quinn and Quinn[11] have recently examined the variation of Vickers hardness with indentation load for a variety of ceramic materials. They observed that the hardness-load curve exhibited distinct transition to a plateau of constant hardness and claimed that such a curve corresponded to the intrinsic hardness value of the materials. In this work, this plateau values for H_D, H_M, and E_r are about 9, 4.3, and 94 GPa, respectively.

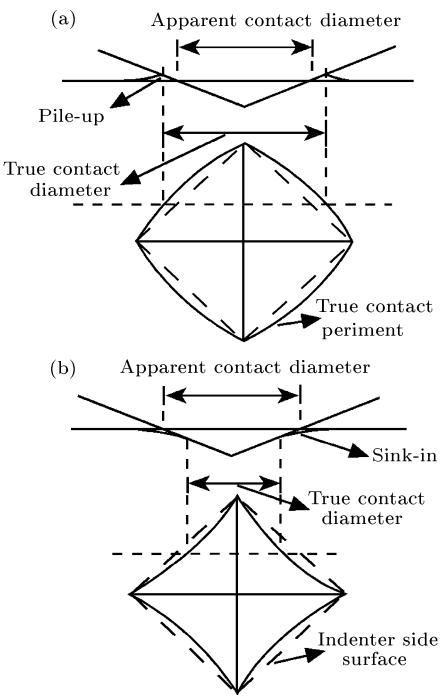

Fig. 7. Schematic illustration of a) pile-up b) sink-in around a sharp indenter.

The indentation load-size effect (ISE) has been examined extensively for microhardness testing of ceramics.[11,12] There have been several explanations for the ISE observed during DSI tests, including

surface pile-up or sinking-in,[13,14] and indenter tip correction.[15] It has been confirmed that for brittle ceramics, it is surface sinking-in rather than pile-up that usually occurs during DSI tests (Fig. 7).[13] Bolshakov *et al.*,[14] reported that the h_f/h_m parameter is a useful indicator of pile-up or sink-in deformation characteristics around the indenter. Pile-up is significant only when h_f/h_m is higher than the critical value (0.7). On the other hand, sink-in behaviour is dominant factor when h_f/h_m is less than the aforementioned critical value, and material shows work hardening deformation behaviour. In Fig. 8, the ratios are shown as a function of indentation load. As can be seen, h_f/h_m values are lower than 0.7 for all the indentation load. The h_f/h_mratios are significantly decreasing with increasing the indentation load. This result implies the existence of sink-in behaviour around to indenter. This finding is also supported by the optical analysis of the Sialon sample (inset in Fig. 8). The figure shows a clear sink-in deformation characteristic around the residual indentation impression for the load-unload indentation experiment.

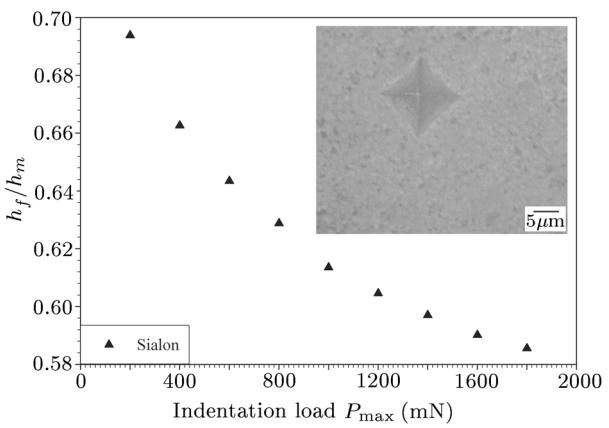

Fig. 8. Ratio between the penetration depth at complete unloading, h_f, and the maximum penetration depth, h_m, as a function of indentation load.

Many attempts have been made to clarify the load dependence and to develop more or less realistic models to interpret hardness tests.[16–18] The empirical equation for describing the ISE is Meyer's law[5,19,20] which uses correlation technique between the test load and the resultant indentation size using a simple power law (Eq. (5)),

$$P_{max} = Ch_c^n, \tag{5}$$

where C and n are constants derived directly from curve fitting of the experimental data. The exponent n, sometimes referred to the Meyer index, is usually considered as a measure of ISE. In summary, the present results indicate that an indentation load effect exists for hardness obtained from DSI tests.

Young's modulus and the hardness were deduced by analysing the unloading segments of the DSI tests load–penetration depth curves using the Oliver–Pharr method. The plastic energy ratio decreases rapidly as the indentation load is increased ranging from 200 to 1800 mN. Both Young's modulus and dynamic, Martens hardness values were exhibit strong indentation load dependence. Consequently, the work-hardening layers, surface-compressed layers, and possibilities for chemical reactions between the atmosphere and the surface, can dominate the yielding mechanism to produce non-standard hardness values.[21] The experimental h_f/h_m ratios lower than the critical value 0.7 indicate that our sample shows work hardening behaviour.

The author is grateful to Professor Malgorzata Sopicka-Lizer from Silesian University of Technology, Katowice, POLAND, for supplying the sample.

References

[1] Jack K H 1976 *Mater. Sci.* **11** 1135
[2] Ziegler G, Heinrich J and Wötting G 1987 *J. Mater. Sci.* **22** 3041
[3] Riley F L 1985 *Sprechsaal.* **118** 225
[4] Greil P and Weiss J 1982 *J. Mat. Sci.* **17** 1571
[5] Şahin O, Uzun O, Kölemen U and Uçar N 2007 *Materials Charac.* (in press) doi:10.1016/j.matchar.2007.02.016
[6] Oliver W C and Pharr G M 1992 *J. Mater. Res.* **7** 1564
[7] Torres F, Benino Y, Fujiwara T and Komatsu T 2004 *Mater. Res. Bull.* **39** 1431
[8] Gong J and Li Y 2000 *J. Mater. Sci.* **35** 209
[9] Galusek D, Riley F L and Riedel R 2001 *J. Am. Ceram. Soc.* **84** 1164
[10] Uzun O, Kölemen U, Çelebi S and Güçlü N 2005 *J. Eur. Ceram. Soc.* **25** 969
[11] Quinn J B and Quinn G D 1997 *J. Mater. Sci.* **32** 4331
[12] Li H and Bradt R C 1993 *J. Mater. Sci.* **28** 917
[13] Zeng K, Söderlund E, Giannakopoulos A E and Rowcliffe D J 1996 *Acta Mater.* **44** 1127
[14] Bolshakov A and Pharr G M 1998 *J. Mater. Res.* **13** 1049
[15] Zong Z and Soboyejo W 2005 *Mater. Sci. Eng.* A **404** 281
[16] Gong J, Zhao Z, Guan Z and Miao H 2000 *J. Eur. Ceram. Soc.* **20** 1895
[17] Sangwall K, Surowska B and Blaziak P 2002 *Mater. Chem. Phys.* **77** 511
[18] Sangwall K, Surowska B and Blaziak P 2003 *Mater. Chem. Phys.* **80** 428
[19] Şahin O, Uzun O, Kölemen U and Uçar N 2007 *J. Phys.: Condens. Matter* **19** 306001
[20] Şahin O, Uzun O, Kölemen U and Uçar N 2007 *Mater. Charac.* (in press) doi:10.1016/j.matchar.2007.06.005
[21] Yurkov A L, Jhuravleva N V and Lukin E S 1994 *J. Mater Sci.* **29** 6551